Soft Matter

COMMUNICATION

Fabrication and stimuli-responsive behavior of flexible micro-scrolls†

Weiming Li,‡ Gaoshan Huang,‡ Hai Yan, Jiao Wang, Ying Yu,* Xinhua Hu, Xiaojing Wu and Yongfeng Mei*

We have fabricated micro-scrolls (tubes/springs) by rolling up pre-strained metal/PVA–PAA bilayers, where the strain is caused by the swelling of the PVA–PAA hydrogel in aqueous media. Stimuli-responsive behavior of the micro-tubes/springs is demonstrated by rolling and unrolling caused by the volume change of the PVA–PAA hydrogel in response to environmental fluids.

In the past few decades, "smart" materials, which show responsive behaviors to external stimuli or their environment, such as pH, temperature, light, solvent composition, humidity and electrical charge,[1–3] have become focused on because of their wide applications in self-healing,[4] displays,[5] biomimetic sensor/actuator devices[6] and micro-opto mechanical systems (MOMS).[7] The materials are normally incorporated into microcantilever-based structures where either the top or bottom of the cantilevers' surfaces is functionalized with "smart" materials to detect target molecules.[8,9] The sensors made from such hybrid microcantilevers have attracted considerable attention during the past few years as they have shown huge potential applications in physical, chemical and biochemical sensing.[10,11] However, the complex manufacturing process of microcantilevers and the corresponding higher cost may hinder their practical applications in routine life.

Recently, a new method to produce 3D micro-/nano-structures, including tubes, rings, wrinkles, springs and other unique structures, has been invented and developed because the fabricated structures can be widely used in electronics, mechanics, robotics and photonics.[12–15] The so-called "self-rolling" technique combines "bottom up" and "top down" approaches, where the pre-strained nanomembranes are sophisticatedly patterned and released from the substrate by a selective etching process.[13–17] In general, the strain in nanomembranes can be deterministically tuned by engaging various mechanisms such as lattice mismatch,[13,16,17] different thermal expansion coefficients between materials,[14,18] or selective swelling of polymers in solvents.[19,20] Naturally, the incorporation of "smart" materials in self-rolled 3D structures[21,22] provides an alternative option to control the strain/stress inside the nanomembranes *in situ*. The tuning ability of the strain and therefore the geometry of the resultant 3D micro-/nano-structures undoubtedly suggest sensing applications of those structures with respect to compositional or environmental stimuli. Compared with traditional cantilever-based sensors, the present self-rolled structures can be easily fabricated and mass-produced in parallel, which is inherent to the self-rolled method, and thus may have great potential in low-cost sensors.

Hydrogels, one of the "smart" materials, can have volumetric changes in response to environmental changes,[1] and thus may be engaged in such 3D self-rolled micro-/nano-sensors. It is worth mentioning that folding and unfolding behaviors of pure polymer bilayers in response to thermal stimuli to encapsulate cells were reported previously.[21,22] Here, in this communication, micro-scrolls, including tubular and helical structures, were successfully fabricated by rolling up metal/polymer bilayers. The rolled-up micro-scrolls (tubes and springs) functionalized by hydrogel layers can detect the environmental changes, mimicking the microcantilever-based sensors. Detailed analyses of the strain status in the flexible micro-scrolls demonstrate that the swelling of polyvinyl alcohol (PVA)–poly(acrylic acid) (PAA) hydrogel in the tube introduces more additional strain than that in the spring because partial strain of springs is released in the perpendicular direction. The flexible micro-scrolls rolled from metal/PVA–PAA bilayer nanomembranes might be designed as simplified solvent composition sensors, which are less complicated and can be easily fabricated compared with previous microcantilever-based sensors.

Fig. 1a illustrates the stimuli-responsive ability of micro-tubes/springs. The "smart" material (hydrogel) is first deposited on the sacrificial layer by dip-coating or spin-coating, which is then followed by the deposition of a metal layer. After lithographic patterning of the bilayer nanomembrane, the sacrificial layer is etched away to release the bilayer to form flexible micro-scrolls due to the volume expansion of the hydrogel. It is worth noting that the inner wall is made of a metal layer while the outer wall consists of a hydrogel. In order to obtain microsprings, the strain/stress inside the nanomembrane must be anisotropic.[23] Here, we adopted glanced angle deposition (GLAD) to introduce anisotropy in the mechanical properties of metal layers and the nanomembrane is patterned into strips misaligned to the preferred rolling direction (the "soft" direction of the anisotropic nanomembrane).[18,24] The inset of Fig. 1a shows a scanning electron microscope (SEM) image of a Ti microspring fabricated by GLAD. The stimuli-responsive behaviors of microtubes and microsprings are illustrated in Fig. 1b. Micro-scrolls can unroll and roll, due to the contraction and expansion of hydrogels respectively, in response to the external stimuli, such as light, pH, temperature or solvent composition depending on the properties of the hydrogel.[1,25] Here, as

Department of Materials Science, Fudan University, Shanghai 200433, People's Republic of China. E-mail: yu_ying@fudan.edu.cn; yfm@fudan.edu.cn; Tel: +86-21-6564 3615

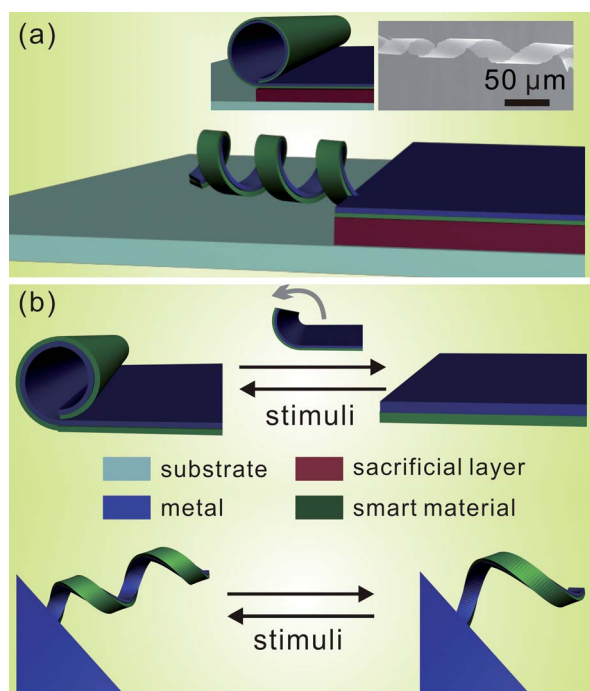‡ These authors contributed equally to this work.

Fig. 1 (a) Schematic illustration of the fabrication of metal/polymer micro-scrolls (tubes/springs). (b) Schematic diagram representing the stimuli-responsive behavior of the microtube (upper) and microspring (down). The inset of Fig. 1a shows the SEM image of a titanium microspring fabricated by GLAD.

a preliminary demonstration, PVA–PAA hydrogel, which has a strong swelling ability and can be obtained by thermal cross-linking,[26] was adopted in our experiments.

Fig. 2a shows a basic process to fabricate bilayer micro-scrolls. PVA and PAA were dissolved separately in de-ionized water at 80 °C (PVA 15 wt% and PAA 7.5 wt%). The solutions were then mixed in a manner that 4 wt% was PVA and 1 wt% was PAA and stirred for

1 h at 60 °C to achieve a homogeneous solution for the following spin-coating process.[27] A PVA–PAA layer with a thickness of ~150 nm was spin-coated on the top of the SiO_2/Si substrate, where the thickness of the SiO_2 layer is 200 nm, followed by a heating process for the thermal crosslinking reaction at 130 °C for 30 min to form a 3D network.[27] The crosslinking reaction is crucial since the PVA–PAA polymer without the heat treatment is easily dissolved in water. Fig. 2b is a cross-sectional SEM image of the fabricated structure described above, which clearly shows the layer structure and the surface morphology of the deposited PVA–PAA layer. After the deposition of the PVA–PAA layer, a 50 nm thick metal layer was fabricated on the top of the polymer layer by e-beam evaporation under high vacuum. Then, windows were made by patterning the final bilayer nanomembrane. 5% HF solution was subsequently used to remove the underneath SiO_2 layer to release the nanomembrane from the substrate. It is worth noting that part of the SiO_2 sacrificial layer was unetched by adjusting the etching time so that the formed flexible micro-scrolls are still fixed at the substrate, which is important to position micro-tubes/springs on a chip for application issue.[18] In the present structure, the PVA–PAA layer swells in water by absorbing H_2O molecules while the metal layer serves as a stiff layer upon exposure to water, which introduces a strain gradient into the metal/PVA–PAA nanomembrane and leads to the self-rolling. Fig. 2c demonstrates the optical microscope images of metal/PVA–PAA micro-scrolls [tubes: (i) Au/PVA–PAA, (ii) Ag/PVA–PAA and (iii) Cr/PVA–PAA; springs: (iv) Au/PVA–PAA, (v) Ag/PVA–PAA and (vi) Cr/PVA–PAA]. The diameter of flexible micro-scrolls ranges from several microns to several tens of microns, while their rotations can be well controlled by the etching process.

The stimuli-responsive behavior of Au/PVA–PAA microtubes was investigated by changing the solvent compositions, and the unrolling and rolling behavior of the bilayer nanomembrane was recorded by a digital video camera and selected frames are shown in Fig. 3a. The nanomembrane rolled into a tube in an aqueous environment as the polymer layer swelled by absorbing water. After being placed into ethanol, the tube started to unroll with decreasing curvature and the
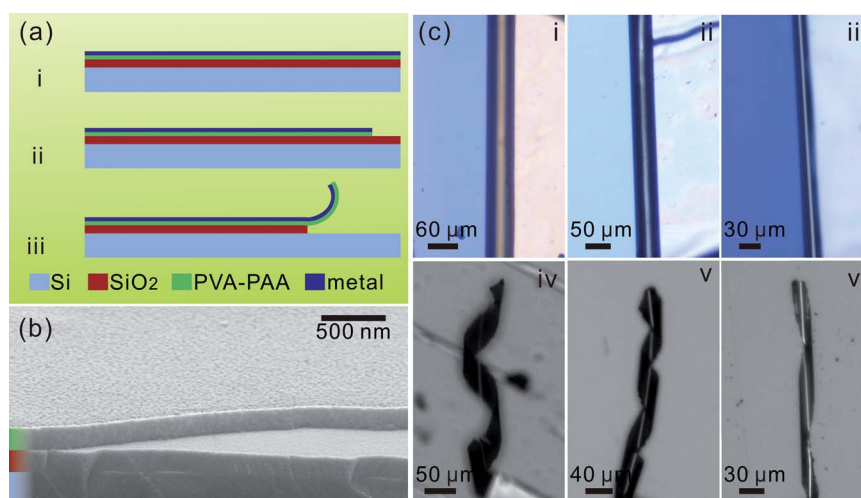

Fig. 2 (a) A basic process to fabricate bilayered micro-scrolls: (i) deposition of the PVA–PAA and metal bilayer, (ii) lithographic patterning, and (iii) releasing process. (b) A cross-sectional SEM image of the PVA–PAA layer on the SiO_2/Si substrate. (c) Optical microscope images of microtubes rolled from the bilayer with the metal layers made of (i) Au, (ii) Cr, and (iii) Ag, respectively, and microsprings with the metal layers made of (iv) Au, (v) Cr, and (vi) Ag respectively.
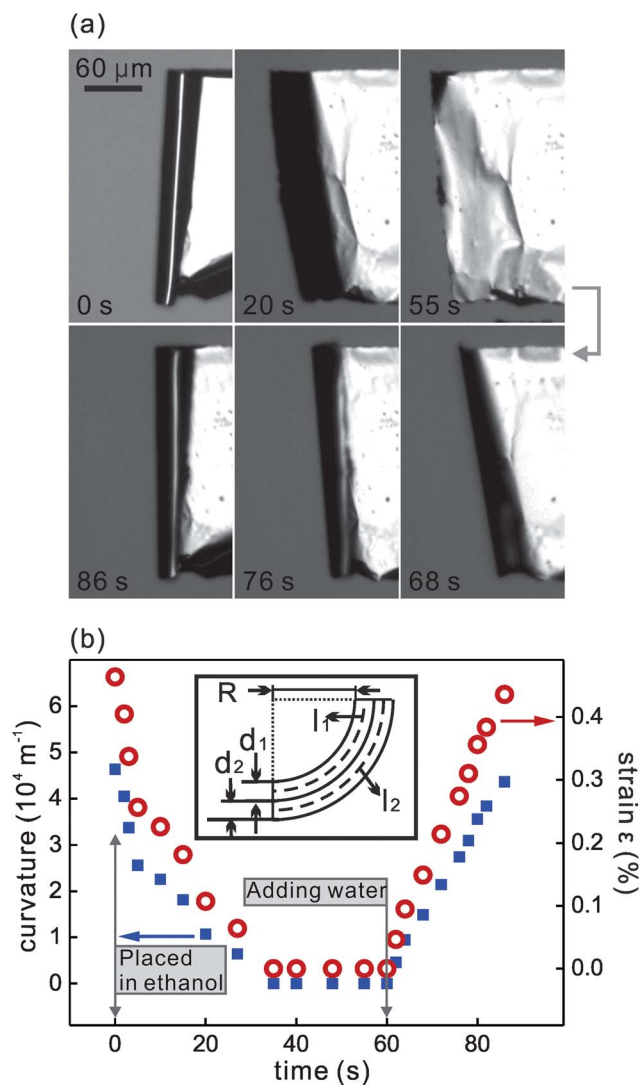
(a)

(b)

Fig. 3 (a) Time profiles of unrolling and rolling motions of an Au/PVA–PAA microtube in different solvents. The microtube was placed into pure ethanol at 0 s, and water was added into the solution at 60 s (the volume ratio of water to ethanol is 1 : 10). (b) Time-dependent curvature of the Au/PVA–PAA microtube and the strain ε derived from the video (see ESI-1-tb.avi†). The inset illustrates the parameters defined for the micro-scroll.

tube even unfolded to an almost flat surface (the curvature is practically zero), because the PVA–PAA hydrogel was dehydrated by ethanol, which led to the deswelling of the polymer layer and the unrolling of the microtube. We noted that if the water content was increased intentionally, the hydrogel can absorb water and swell again, and the nanomembrane restored the tubular shape. Fig. 3b shows the curvature of the Au/PVA–PAA microtube as a function of time derived from the recorded video. When immersed into ethanol, the microtube unrolled to a flat surface in ~35 s with curvature decreasing from 4.63×10^4 m^{-1} to 0 (flat surface). On the other hand, the recovery process took ~25 s after adding water to ethanol (the volume ratio of water to ethanol is 1 : 10). The curvature is thus increased from 0 (flat surface) to 4.36×10^4 m^{-1}. The final radius decreased to 22.9 μm, which is almost the same as that of the initial microtube.

Microsprings rolled from the metal/PVA–PAA nanomembrane exhibit a similar stimuli-responsive behavior as well. The number of cycles in the microspring changed in response to different solvents and the rolling and unrolling behavior of a Cr/PVA–PAA microspring was recorded (see the video: ESI-2-sp.wmv†), which is similar to the situation of tubes. Fig. 4a shows the unrolling and rolling of a microspring in solvent with changing concentration. The Cr/PVA–PAA microspring started to unroll when placed in ethanol and the microspring deformed from 1.45 to 0.4 cycles while the radius increased from 19.0 to 68.9 μm. It is worth noting that the bilayer strip still maintained its helical shape instead of a straight strip while the Au/PVA–PAA microtube unrolled into an almost flat nano-membrane (see Fig. 3a). The key point leading to this difference is considered to be the intrinsically strained Cr layer.[18] The Cr layer is pre-strained during the deposition process, suggesting that the pure Cr layer itself is capable to roll without the assistance of the polymer layer. The morphology of the microspring was restored with radius decreased to 19.0 μm and the number of cycles increased to 1.45 after water was added to the ethanol. The mechanism of rolling and
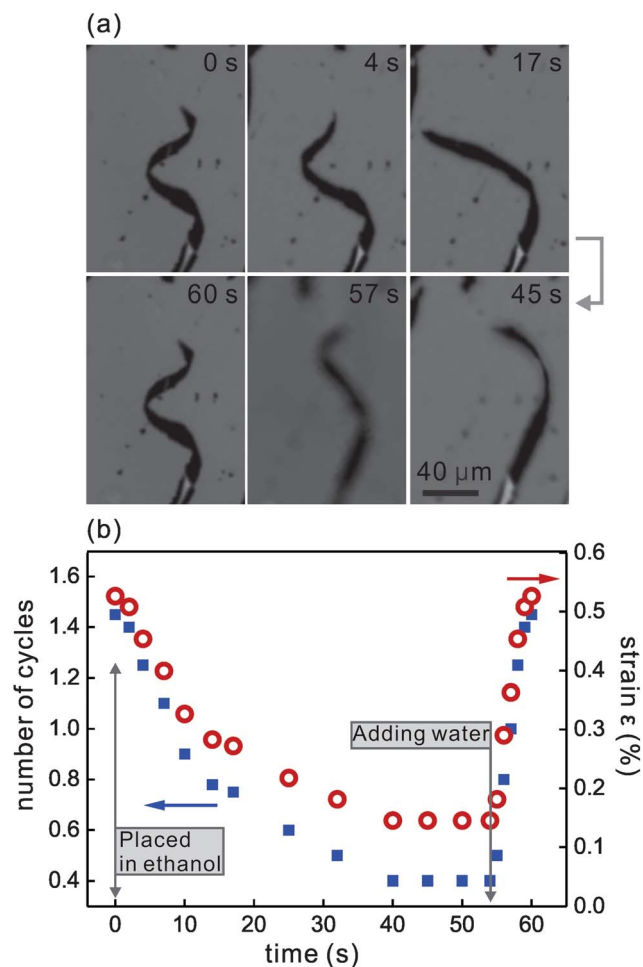
(a)

(b)

Fig. 4 (a) Time profiles of unrolling and rolling motions of a Cr/PVA–PAA microspring in different solvents. The microspring was placed into pure ethanol at 0 s, and water (the volume ratio of water to ethanol is 1 : 10) was added into the solution at 54 s. (b) Time-dependent number of cycles in a Cr/PVA–PAA microspring and the strain ε derived from the video: ESI-2-sp1.wmv†.

unrolling of the microspring should be similar to that in the micro-tube: the contraction and expansion of the PVA–PAA layer in ethanol and water, respectively, cause the observed geometrical evolution. The number of cycles in the microspring as a function of time is shown in Fig. 4b. It took about 40 s for the unrolling process and the recovery process (rolling back) was completed within ∼6 s.

To further investigate the stimuli-responsive behavior of our flexible micro-scrolls, the morphological evolution of an Au/PVA–PAA microtube with respect to solvent composition was recorded. Fig. 5 shows the relationship between the curvature of the microtube and the volume ratio of water to ethanol. The change of the solvent concentration is accomplished step by step and the curvature is calculated based on the image recorded when the geometrical evolution is stabilized. The bilayer nanomembrane was flat when immersed into pure ethanol and the curvature is thus determined to be 0, as shown in Fig. 5. With gradually increasing the water concentration, the nanomembrane started to roll up due to the swelling of the polymer layer by absorbing water. It can be found that when the ratio increased to ∼7%, the increase of curvature became saturated and the nanomembrane rolled into a tight tube, which indicates that the swelling of the PVA–PAA layer reached the maximum.[28]

The strain inside the bilayer nanomembrane and its evolution during the rolling process were investigated in detail based on our microscopy characterization of the microtube, which gives us a clue to estimate the additional strain of the PVA–PAA hydrogel generated by swelling in water. Assuming that the length of the metal layer remains constant during the deformation, the practical strain ε, which causes the rolling, is defined as follows:[29]

$$\varepsilon = \frac{l_2 - l_1}{l_1}, \tag{1}$$

where l_1 and l_2 are, respectively, the length of the metal layer and polymer layer, as illustrated in the inset of Fig. 3b. Assuming that the thickness of the polymer layer remains constant and the radius of the microtube is much larger than the layers' thicknesses, eqn (1) can be written as:
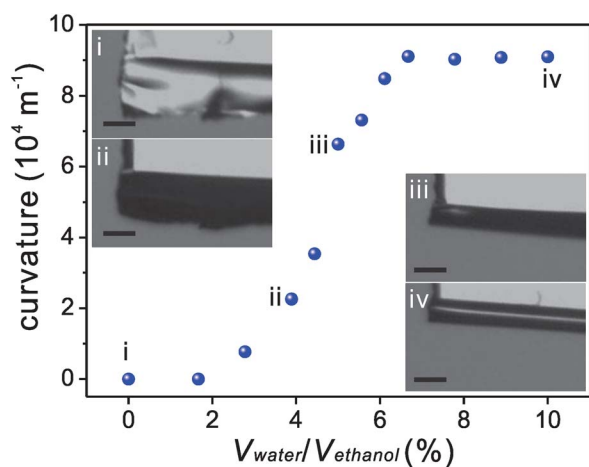

Fig. 5 Curvature of the Au/PVA–PAA microtube in mixed solution as a function of the volume ratio of water to ethanol ($V_{water}/V_{ethanol}$). The insets show the corresponding optical microscope images of microtubes in solutions with different $V_{water}/V_{ethanol}$. The scale bar is 30 μm.

$$\varepsilon = \frac{d_1 + d_2}{2R} \tag{2}$$

where d_1 and d_2 represent the thicknesses of the metal and polymer layers respectively, i.e. 50 nm and 150 nm in the present case, and R is the curved radius of the micro-scroll. Therefore, we can calculate the evolutions of the practical strains in the microtube and microspring during the unrolling and rolling process respectively as shown in Fig. 3b and 4b.

When the metal/PVA–PAA bilayer nanomembrane is immersed into water, the polymer layer absorbs water and swells. To illustrate this quantitatively, here we propose a method to estimate the nominal strain of the hydrogel layer after swelling. Please note that this nominal strain reflects the property of the hydrogel itself, which cannot be directly observed because the hydrogel layer is bonded to the metal layer and only the practical strain ε is presented (see eqn (1) and (2)). The radius of a rolled-up structure R can be estimated by the following equation:[29,30]

$$R = \frac{(d_1 + d_2')\left\{3\left(1 + \frac{d_1}{d_2'}\right)^2 + \left(1 + \frac{d_1}{d_2'} \bullet \frac{Y_1}{Y_2}\right)\left[\left(\frac{d_1}{d_2'}\right)^2 + \left(\frac{d_1}{d_2'} \bullet \frac{Y_1}{Y_2}\right)^{-1}\right]\right\}}{6\varepsilon'\left(1 + \frac{d_1}{d_2'}\right)^2} \tag{3}$$

where d_2' is the thickness of the swollen polymer layer, Y_1 and Y_2 are the Young's moduli of the metal layer and polymer layer respectively, and ε' is the nominal strain along the rolling direction. It is noted that the ε' consists of the strain of the metal layer produced during the deposition and the strain of the swollen polymer. Thus, ε' can be expressed as:

$$\varepsilon' = \varepsilon_p' + C \tag{4}$$

where ε_p' represents the strain from the swelling of the polymer layer and C represents the strain contributed by the metal layer which remains constant during the deformation process.

In our simplified model, the Young's moduli for Au, Cr and PVA–PAA are assumed to be constant during the deformation, i.e. 79 GPa,[31] 279 GPa,[32] and 1.38 MPa,[25] respectively. The thickness of the polymer layer d_2' increases as the polymer swells and it is assumed that it can be determined by ε_p' as follows:

$$d_2' = d_2\left(1 + \varepsilon_p'\right) \tag{5}$$

Considering the huge difference in Young's moduli, eqn (3) can be simplified as:

$$R = \frac{d_1^3}{6\varepsilon'\left(d_1 + d_2'\right)d_2'} \bullet \frac{Y_1}{Y_2} \tag{6}$$

Combining eqn (4) and (5), eqn (6) can be written as:

$$R = \frac{d_1^3}{6\left(\varepsilon_p' + C\right)\left[d_1 + d_2\left(1 + \varepsilon_p'\right)\right]d_2\left(1 + \varepsilon_p'\right)} \bullet \frac{Y_1}{Y_2} \tag{7}$$

The constant C can be calculated in the situation when no water is absorbed and thus ε_p' is set to zero. Fig. 6 shows the evolution of ε_p' as a function of swelling time, deduced from the real-time videos by using eqn (7). The ε_p' decreased when micro-scrolls were transferred to ethanol due to the contraction of the hydrogel (dehydrated by the ethanol). It is noted that when the polymer reaches its maximum
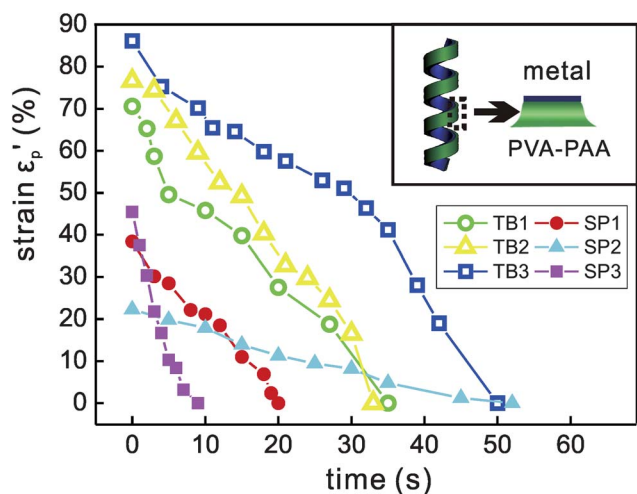
Fig. 6 Evolution of strains inside the polymer layers (ε_p') in microtubes and microsprings. TB1, TB2 and TB3 represent three different Au/PVA–PAA tubes, and SP1, SP2 and SP3 represent three different Cr/PVA–PAA microsprings. The inset illustrates the swelling of the polymer layer vertical to the strip direction in a microspring structure.

degree of swelling, *i.e.* before being transferred to ethanol, ε_p' of the microtube is estimated to be 70–86% while that of the microspring is only 22–45%. The strain of the polymer layer in microtubes is obviously larger than that of microsprings. This is because the partial strain of the hydrogel in microsprings is relaxed perpendicular to the rolling direction and along its surface in the case of narrow strips, which was also observed in the fabrication of SiGe/Si and SiGe/Si/Cr microsprings.[23] Different from tubes, springs are rolled from strips with a narrow width and the polymer layer swells vertically to the direction of the strip as depicted in the inset of Fig. 6, this geometrical effect consequently leads to partial strain relaxation.[23,33,34]

In conclusion, flexible micro-scrolls were fabricated by rolling up metal/PVA–PAA bilayers, which were prepared by evaporating a metal layer on top of a thermally crosslinked PVA–PAA layer. Based on the swelling property of the PVA–PAA hydrogel in aqueous media, a stimuli-responsive behavior of fabricated micro-scrolls was noticed as a reversible rolling and unrolling action. The detailed investigation on the strain status of the hydrogel layer demonstrates that the nominal strain in microtubes is always larger than that in microsprings due to the partial strain relaxation perpendicular to the rolling direction in microsprings. The ability of the micro-scrolls to roll or unroll due to the expansion or contraction of the polymer layer in response to different solvents suggests that the micro-tubes/springs can be potentially applied in *e.g.* sensing, actuating and cells encapsulation.[35]

Acknowledgements

Notes and references

1 I. Tokarev and S. Minko, *Soft Matter*, 2008, **5**, 511–524.
2 Y. Yu, M. Nakano and T. Ikeda, *Nature*, 2003, **425**, 145.
3 M. Yoshida and J. Lahann, *ACS Nano*, 2008, **2**, 1101–1107.
4 S. H. Cho, H. M. Andersson, S. R. White, N. R. Sottos and P. V. Braun, *Adv. Mater.*, 2006, **18**, 997–1000.
5 B. Comiskey, J. Albert, H. Yoshizawa and J. Jacobson, *Nature*, 1998, **394**, 253–255.
6 J. Kim, S. Yun and Z. Ounaies, *Macromolecules*, 2006, **39**, 4202–4206.
7 Y. Zhao and T. Ikeda, *Smart Light-Responsive Materials: Azobenzene-Containing Polymers and Liquid Crystals*, Wiley, 2009.
8 A. Boisen, S. Dohn, S. S. Keller, S. Schmid and M. Tenje, *Rep. Prog. Phys.*, 2011, **74**, 036101.
9 C. Jiang and V. V. Tsukruk, *Adv. Mater.*, 2006, **18**, 829–840.
10 S. Singamaneni, M. C. LeMieux, H. P. Lang, C. Gerber, Y. Lam, S. Zauscher, P. G. Datskos, N. V. Lavrik, H. Jiang, R. R. Naik, T. J. Bunning and V. V. Tsukruk, *Adv. Mater.*, 2008, **20**, 653–680.
11 V. Seena, A. Nigam, P. Pant, S. Mukherji and V. R. Rao, *J. Microelectromech. Syst.*, 2012, **21**, 294–301.
12 J. Rogers, M. Lagally and R. Nuzzo, *Nature*, 2011, **477**, 45–53.
13 O. G. Schmidt and K. Eberl, *Nature*, 2001, **410**, 168.
14 Y. F. Mei, A. A. Solovev, S. Sanchez and O. G. Schmidt, *Chem. Soc. Rev.*, 2011, **40**, 2109–2119.
15 L. Zhang, K. E. Peyer and B. J. Nelson, *Lab Chip*, 2010, **10**, 2203–2215.
16 I. S. Chun, A. Challa, B. Derickson, K. J. Hsia and X. Li, *Nano Lett.*, 2010, **10**, 3927–3932.
17 F. Liu, M. G. Lagally and J. Zang, *MRS Bull.*, 2009, **34**, 190.
18 Y. F. Mei, G. S. Huang, A. A. Solovev, E. B. Ureña, I. Mönch, F. Ding, T. Reindl, R. K. Y. Fu, P. K. Chu and O. G. Schmidt, *Adv. Mater.*, 2008, **20**, 4085–4090.
19 K. Kumar, B. Nandan, V. Luchnikov, E. B. Gowd and M. Stamm, *Langmuir*, 2009, **25**, 7667–7674.
20 S. Zakharchenko, E. Sperling and L. Ionov, *Biomacromolecules*, 2011, **12**, 2211–2215.
21 G. Stoychev, N. Puretskiy and L. Ionov, *Soft Matter*, 2011, **7**, 3277–3279.
22 Leonid Ionov, *Soft Matter*, 2011, **7**, 6786–6791.
23 L. Zhang, E. Ruh, D. Grützmacher, L. Dong, D. J. Bell, B. J. Nelson and C. Schönenberger, *Nano Lett.*, 2006, **6**, 1311–1317.
24 W. M. Li, G. S. Huang, X. J. Wu and Y. F. Mei, CN patent application, 201110262186.4, 2011.
25 G. Gerlach, M. Guenther, J. Sorber, G. Suchaneck, K. F. Arndt and A. Richter, *Sens. Actuators, B*, 2005, **111–112**, 555–561.
26 J. Sorber, G. Steiner, V. Schulz, M. Guenther, G. Gerlach, R. Salzer and K. F. Arndt, *Anal. Chem.*, 2008, **80**, 2957–2962.
27 A. Richter, A. Bund, M. Keller and K. F. Arndt, *Sens. Actuators, B*, 2004, **99**, 579–585.
28 K. F. Arndt, D. Kuckling and A. Richter, *Polym. Adv. Technol.*, 2000, **11**, 496–505.
29 P. O. Vaccaro, K. Kubota and T. Aida, *Appl. Phys. Lett.*, 2001, **78**, 2852–2854.
30 I. Chun, V. Verma, V. Elarde, S. Kim, J. Zuo, J. Coleman and X. Li, *J. Cryst. Growth*, 2008, **310**, 2353–2358.
31 C. Liang, *Development of Bulk-Scale and Thin Film Magnetostrictive Sensor*, ProQuest, 2007.
32 J. Lintymer, J. Gavoille, N. Martin and J. Takadoum, *Surf. Coat. Technol.*, 2003, **174–175**, 316–323.
33 S. Alebn, B. Balakrisnan and E. Smela, *Nano Lett.*, 2011, **11**, 2280.
34 I. S. Chun, A. Challa, B. Derickson, K. J. Hsia and X. Li, *Nano Lett.*, 2010, **10**, 3927.
35 G. S. Huang and Y. F. Mei, *Adv. Mater.*, 2012, **24**, 2517.

Addition and correction

Note from RSC Publishing

This article was originally published with incorrect page numbers. This is the corrected, final version.

The Royal Society of Chemistry apologises for these errors and any consequent inconvenience to authors and readers.